



# How to mimic the thermo-induced red to green transition of ruby with control of the temperature via the use of an inorganic materials blend?

M. Gaudon<sup>a,\*</sup>, P. Deniard<sup>b</sup>, L. Voisin<sup>c</sup>, G. Lacombe<sup>a</sup>, F. Darnat<sup>a</sup>, A. Demourgues<sup>a</sup>, J.-L. Perillon<sup>c</sup>, S. Jobic<sup>b</sup>

<sup>a</sup> CNRS, Université de Bordeaux, ICMCB, 87 Avenue du Dr. Albert Schweitzer, 33608 Pessac Cedex, France

<sup>b</sup> Institut des Matériaux Jean Rouxel, Université de Nantes, CNRS, 2 rue de la Houssinière, BP 32229, 44322 Nantes Cedex 3, France

<sup>c</sup> Tefal SA, Chemin des Granges, 74150 Rumilly, France

## ARTICLE INFO

### Article history:

Received 29 November 2011

Received in revised form

22 March 2012

Accepted 30 April 2012

Available online 22 May 2012

### Keywords:

Inorganic pigment

Semiconductor

d-d Transition

Oxides

Thermochromism

Subtractive synthesis

## ABSTRACT

The design of new smart pigments with a strong colour change in a given temperature ( $T$ ) range turns out to be often very time-consuming and costly. Based on this observation, we propose here a cheap solution consisting in the mixing in appropriate amounts of a semiconductor and a d-d transition based pigment. The former exhibits a strong temperature dependence of its optical gap while the second presents a null or moderate evolution of the positioning of its absorption band with  $T$ . This results in the generation of various reversible thermochromic effects with control of both the temperature transition and the hue in the low and high temperature stages. An example will be devoted to the reproduction of the  $\text{Al}_{2-x}\text{Cr}_x\text{O}_3$  corundum behaviour in the 20–200 °C domain with a  $\text{Bi}_2\text{O}_3$ – $\text{LiCoPO}_4$  blend. The proposed recipe, easily extrapolated to a wide range of colour changes, is only based on the well known subtractive colouring model, and the evolution of the chromatic coefficients of each ingredient with  $T$ . This opens up the door to the development of a new generation of thermochromic pigments with unsaturated colours for potential applications as temperature indicators.

© 2012 Elsevier Ltd. All rights reserved.

## 1. Introduction

Thermochromic materials are materials which colour changes upon cooling or heating [1–6]. This property concerns both organic and inorganic substances but only inorganic compounds will be discussed in the following for convenience. Thermochromism is a very exciting phenomenon because it is observed with naked eyes and can give rise to many applications, not only as temperature indicators for fun (smart textile, cosmetics, paints...) but also as smart pigments to fight against counterfeiting (security inks for money, clothing, watches, software and pharmaceutical packaging...), danger alert markers (hot-plates, alarm sign for thermo-mechanical fatigue in turbine engines or gas turbines, cold chain rupture...), and cheap switchable glasses with automatic control of the light transmission under solar illumination induced heating... The colour change can be continuous or abrupt with temperature, reversible or irreversible depending on the nature of the materials, the temperature range and the colour origin. By essence, it has to be emphasized the fact that any pigments and coloured inorganic compounds can give rise to thermochromism since colour is

associated with electronic transitions from a ground state to an excited state which position in energy are correlated to the electronic charge distribution in the solid, i.e. the contraction/expansion of the inter-atomic distances. The inorganic pigments are mainly coloured from two different electronic transfers [2,7–9]: (i) intra-atomic transfer occurring in transition metals, for instance, while they are submitted to a ligand field inducing d-orbitals splitting, (ii) inter-atomic electronic transfers as occurring in semiconductors considering the electronic charge transfers between the oxygen anions and the cations can be schematized by band diagrams.

For intrinsic (undoped) semiconductors, colour originates from the promotion of electrons from the valence band to the conduction band. For such materials, the hue can move from black to red, orange, yellow and white versus the energy gap. Violet, blue, cyan and green colours cannot be generated in such materials except via the insertion of defects or dopants. As the optical gap is commonly directly related to orbital overlaps between the constituents, a temperature-induced volume expansion will go along with longer inter-atomic distances, a lesser covalence of the chemical bonds, and a regular decrease of the optical gap with temperature. Hence, the continuous shift from yellow (at 20 °C) to red (at 300 °C) in  $\text{BiVO}_4$  can be explained for instance. Theoretically, the inverse effect, i.e. an increase of the gap with  $T$ , could appear for few

\* Corresponding author.

E-mail address: [gaudon@icmcb-bordeaux.cnrs.fr](mailto:gaudon@icmcb-bordeaux.cnrs.fr) (M. Gaudon).

materials with negative expansion coefficients. Practically, the major drawback of semiconducting materials lies in the difficulty to associate a temperature with a hue with a good accuracy even with the use of a colours chart.

For the materials with intra-atomic parity forbidden d-d transitions, the crystal field is directly influenced by the thermal expansion. The archetype of such a material is  $\text{Cr}^{3+}$  doped  $\alpha\text{-Al}_2\text{O}_3$  which exhibits the ability to transit from red to green (via a very brief intermediate grey state) upon warming at a well defined temperature depending only on the Cr:Al ratio. Hence, according to Akabori and Kushi [2], the colour change may take place between  $-183^\circ\text{C}$  and  $377^\circ\text{C}$  for Cr concentrations ranging between 58% and 2%, respectively. This green to red colour change via a grey intermediate hue is plenty efficient besides human eye vision [10]. So far, this colour change is associated with a displacement towards low energies of the  ${}^4\text{A}_2 \rightarrow {}^4\text{T}_2$  and  ${}^4\text{A}_2 \rightarrow {}^4\text{T}_1$  spin allowed transitions with temperature in relation with a decrease of the ligand field splitting of the  $\text{Cr}^{3+}$  d-orbitals directed by an enhancement of the Cr–O inter-atomic distances [2,11,12]. Unfortunately, the low refractive index of  $\alpha$ -alumina coupled to the weak oscillator strength of the  $\text{Cr}^{3+}$  parity forbidden d-d transitions of powdered red ruby lead to pale colours without major interest for industrial applications.

Besides, thermal expansion, phase transitions produce a thermochromic phenomenon. Namely, a large number of mercury containing salts exhibits the propensity to transit towards a new allotropic form with temperature with significant change in the structure arrangement leading to an important colour change. Let mention for instance  $\text{HgI}_2$  which shifts from red to yellow at  $127^\circ\text{C}$ ,  $\text{Ag}_2\text{HgI}_4$  which transits from a yellow state to an orange one at  $50^\circ\text{C}$ , etc. Nevertheless, the most developed thermochromic pigments based on this phase transition phenomenon remains, without any doubt, vanadium dioxide and its doped derivatives. These materials received much attention due to their potential application as thermal insulator coatings in smart windows in connection with a reversible temperature driven insulator-metallic transition [13–19]. More recently, the authors reported investigations on  $\text{AMoO}_4$  compounds and their W doped derivatives ( $\text{A} = \text{Cu}, \text{Co}$ ). These materials evidence very interesting thermochromic (and tribochromic) properties in relation with change of the coordination number of molybdenum at the transition temperature. Unfortunately, they exhibit a poor cyclability: a material with high cyclability being a material which can be used many times without properties deterioration. Herein, the poor cyclability is likely assigned to a too large cell expansion (contraction) at the transition under heating (cooling). This causes cracks within grains which finally lead to the stabilization of the high temperature form only after several heating/cooling cycles [20–26]. In brief, the major limitations of thermochromic materials based on a phase transition concerns usually their natural temperature hysteresis (transition temperatures on heating and cooling different) and their propensity to fatigue under cycling.

Even if smart pigments have been intensively investigated, it remains a hard task to anticipate the evolution of the chromatic coefficients of inorganic materials with temperature. In other terms, this makes complicated the *ex-nihilo* design of new thermochromic pigments for specific applications with harsh requisites concerning the temperature transition and the colour characteristics in the low and high temperature state in a given temperature domain. This leads us to propose a simple model to prepare reversible and cyclable thermochromic mixtures. Our choice was made on the assembly of a semiconductor and a d-d transition based pigment, the former exhibiting an *a priori* strong temperature dependence of its optical gap while the latter presenting a null or a moderate evolution of the positioning of its absorption band. In

the following, we will illustrate the setting-up procedure to reproduce the red to green transition of ruby for a potential application at  $200^\circ\text{C}$ . This red to green change is of a capital importance in our every day life, the green and the red colours symbolizing in the collective unconscious permission and interdiction, respectively. Our approach may be easily extrapolated to others requisites by choosing the appropriate pigments in the right amounts. This will lead systematically to unsaturated colours, but contrasts are sufficient when heated or cooled to be distinguishable with naked eyes. In the coming paragraphs, we will report on the thermochromic effect of  $\text{Bi}_2\text{O}_3\text{--CoAl}_2\text{O}_4$  and  $\text{Bi}_2\text{O}_3\text{--LiCoPO}_4$  mixtures which shift from cyan to green and from magenta to green, respectively. Thereafter we will extend our investigation to the  $\text{V}_2\text{O}_5/\text{Cr}_2\text{O}_3$  mixture which transits from red to green with  $T$ . This highlights the multiple possible extensions based on our reasoning.

## 2. Background

Based on the subtractive colour synthesis principle, it is well known that the combination of a yellow pigment with a cyan one can lead to a green mixture with a colour strength depending on the relative ratio of the ingredients. In a similar way, the combination of a yellow pigment with a magenta one can generate a red mixture. Let us now mix a white or yellow pale pigment, namely a semiconductor with an optical gap of 3.0 eV, with magenta or cyan pigments. Then, the colour of the blend should shift from pale magenta or pale cyan to red or green with temperature, respectively, the optical gap of the white pigment decreasing of about 0.2 eV going from  $20^\circ\text{C}$  to  $200^\circ\text{C}$ . Namely, for almost semiconductors, the optical gap is submitted to a red-shift when heated (the colour is shifted according to the sequence white  $\rightarrow$  yellow  $\rightarrow$  orange  $\rightarrow$  red  $\rightarrow$  black). Experimental models have been proposed to account for the evolution of the forbidden gap ( $E_g$ ) with temperature ( $T$ ) in these materials. Hence, Varshni suggested a fit of the  $E_g(T)$  curve with the equation,  $E_g(T) = E_g(0) - \frac{AT^2}{T+B}$ , where  $E_g$  and  $T$  are expressed in eV and K,  $E_g(0)$  is the optical gap at 0 K, and  $A$  and  $B$  are adjustable semi-empirical values depending on the considered material. [27–29]. Typically we estimate that a variation of 0.10–0.15 eV of  $E_g$  per 100 K difference is reasonable. This is a change of colouration versus temperature clearly more important than the one observed in ruby in the 0–400  $^\circ\text{C}$  temperature estimated around 0.02 eV [1,2]. Thus, the temperature-induced colour change is supposed to be much more pronounced in a semiconductor than in coloured compounds where d-d transitions are at work. In the following, we have chosen  $\text{Bi}_2\text{O}_3$  as the white pigment.

What about the choice of the cyan and magenta pigments? It is interesting to notice that the colours of cobalt II ( $d^7_{\text{HS}}$  configuration) based pigments strongly depends upon the coordination of the chromophore. Commonly, pink to purple hues are associated with cobalt in octahedral coordination (e.g.  $\text{LiCoPO}_4$ ), while the blue colour is generated by cobalt at tetrahedral site (e.g.  $\text{CoAl}_2\text{O}_4$ ). Reflectance spectra of compounds with Co ions in octahedral site are commonly characterized by a broad absorption band around 560 nm assigned to a  ${}^4\text{T}_{1g} \cdot ({}^5\text{e}_g^2) \rightarrow {}^4\text{T}_{1g} \cdot ({}^4\text{t}_g^3\text{e}_g^3)$  transition splitting into bundles due to multiplet coupling [30–34]. The  ${}^4\text{T}_{1g} \cdot ({}^5\text{e}_g^2) \rightarrow {}^4\text{A}_{2g}({}^3\text{t}_g^3\text{e}_g^4)$  and  ${}^4\text{T}_{1g} \cdot ({}^5\text{e}_g^2) \rightarrow {}^4\text{T}_{2g} \cdot ({}^4\text{t}_g^3\text{e}_g^3)$  transitions do not contribute to the colour, the former being a two electron transition, the latter being systematically localized in the near infra-red. Samples with cobalt at tetrahedral sites exhibit usually three absorption bands peaking at about 550, 580 and 620 nm assigned to  ${}^4\text{A}_2 \cdot ({}^4\text{t}_2^3) \rightarrow {}^4\text{T}_2 \cdot ({}^3\text{e}^3\text{t}_2^3)$ ,  ${}^4\text{A}_2 \cdot ({}^4\text{t}_2^3) \rightarrow {}^4\text{T}_1 \cdot ({}^3\text{e}^3\text{t}_2^3)$  and  ${}^4\text{A}_2 \cdot ({}^4\text{t}_2^3) \rightarrow {}^4\text{T}_1 \cdot ({}^2\text{e}^2\text{t}_2^5)$ , respectively [38,39]. Due a lesser hybridization of the d-orbitals of Cobalt and those of the ligand, the

position change of the absorption bands of the chromophore are less impacted with  $T$  than in semiconductors, even if the Tanabe and Sugano diagram suggests a red-shift when  $T$  increases. Moreover, we may predict that the colour change with  $T^\circ$  (if it exists) will be more pronounced for octahedral sites than for tetrahedral sites due to a lesser covalence (rigidity) of the metal-ligand bonds for octahedra than for tetrahedra, and because the ligand field splitting of octahedral sites is almost two times superior to the ligand field splitting of tetrahedral sites (which suggests that a small change in the inter-atomic distance will have more impact).

### 3. Experimental

#### 3.1. Synthesis

All raw materials used are purchased from Aldrich.  $\text{CoAl}_2\text{O}_4$  was synthesized by solid-state route from  $\alpha\text{-Al}_2\text{O}_3$  and  $\text{Co}_3\text{O}_4$  at  $1200^\circ\text{C}$  for 20 h.  $\text{LiCoPO}_4$  was prepared from  $\text{Li}_2\text{CO}_3$ ,  $\text{Co}_3\text{O}_4$  and  $(\text{NH}_4)\text{H}_2\text{PO}_4$  at  $800^\circ\text{C}$  for 12 h. The chemical and structural behaviour of the spinel oxide and lithium–cobalt phosphate were already fully characterized (via XRD, ICP...) in previous authors' works [35–37].

#### 3.2. Reflectivity measurements at RT

Room temperature UV–vis diffuse reflectivity spectra were collected from a finely ground sample on a Cary 5G spectrometer (Varian). This instrument was equipped with a 60 mm diameter, polytetrafluorene coated integrating sphere. Diffuse reflectivity was measured from 200 to 2000 nm with a 1 nm step using Halon powder (from Varian) as reference (100% reflectance). The absorption ( $\alpha/S$ ) data were calculated from the reflectivity using the Kubelka-Munk transformation:  $\alpha/S = (1 - R)^2/2R$ , where  $R$  is the reflectivity at a given wavelength,  $\alpha$  is the absorption coefficient, and  $S$  is the scattering coefficient. The latter was supposed to be particle size independent, as expected for particles with diameter larger than a few micrometres. Practically, optical gaps were determined after a Kubelka-Munk (KM) transformation of the reflectivity spectrum as the intersection point between the energy axis and the line extrapolated from the linear portion of the absorption threshold.

#### 3.3. Temperature dependent reflectivity measurements

The evolution of the reflectivity with temperature of  $\text{Bi}_2\text{O}_3$ ,  $\text{CoAl}_2\text{O}_4$  and  $\text{LiCoPO}_4$  was carried with a home-built instrument equipped with a CVI spectrometer equipped with a tubular furnace. Time-of-fly acquisition was monitored in the 400–1000 nm region at a  $2\text{ K min}^{-1}$  heating rate.

#### 3.4. Determination of the chromatic parameters

Powders were deposited on a hot-plate and  $L^*a^*b^*$  parameters were calculated from RT up to  $200^\circ\text{C}$  with a Konica-Minolta CM-700d spectrophotometer equipped with a PTFE coated integrating sphere. A white calibration cap CM-A177 (ceramic) and the standard D65 (Daylight, colour temperature = 6504 K) with a  $10^\circ$  observer angle (CIE Konica-Minolta1964) were used as the white reference and illuminant, respectively.

### 4. Results and discussion

$\text{Bi}_2\text{O}_3$  is a wide gap semiconductor with a pale yellow colouration and a steep absorption threshold at about 2.8 eV at room temperature. The evolution of its reflectance spectrum with

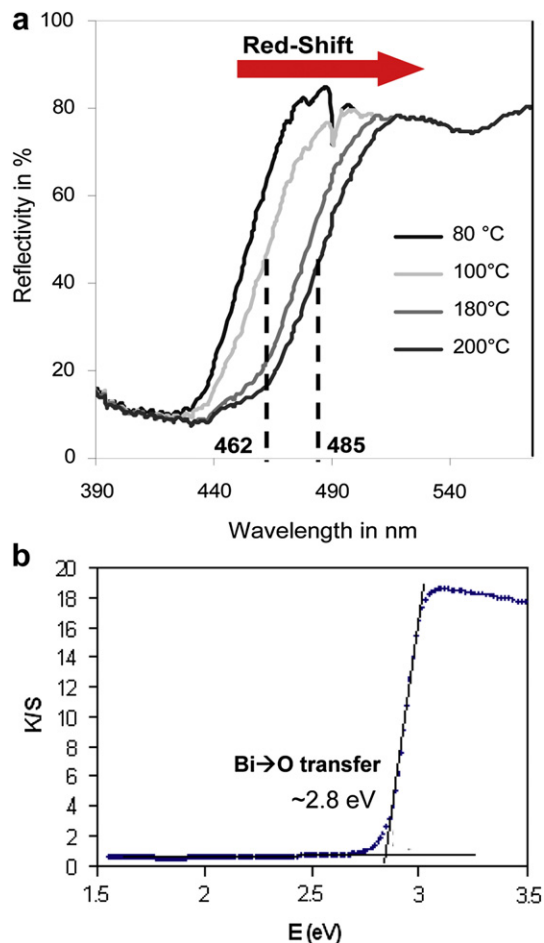





**Fig. 1.** (a) Evolution of the reflectance spectra of  $\text{Bi}_2\text{O}_3$  versus temperature between room and  $200^\circ\text{C}$ . (b) Kubelka-Munk transformed reflectance spectrum of  $\text{Bi}_2\text{O}_3$  at room temperature.




temperature is given in Fig. 1a for increasing temperatures up to  $200^\circ\text{C}$  with the KM transformation at room temperature in Fig. 1b. A gap decrease rate of  $1.3\text{ eV}/^\circ\text{C}$  can be calculated. The chromatic coefficients of  $\text{Bi}_2\text{O}_3$  at 20, 100 and  $200^\circ\text{C}$  are given in Table 1.

The KM transformed spectra of  $\text{CoAl}_2\text{O}_4$  and  $\text{LiCoPO}_4$  at room temperature are displayed in Fig. 2. Spectra evidence the aforementioned characteristic features of  $\text{Co}^{2+}$  cations with a  $d^7$  high spin configuration for tetrahedral and octahedral sites, respectively. The evolution of  $R(T)$  for  $\text{CoAl}_2\text{O}_4$  is not significant. At the opposite,  $\text{LiCoPO}_4$  presents an enlargement of the d-d absorption band with temperature (Fig. 3): the absorption band ranging from 480 to 620 nm at room temperature progressively encroaches on the orange domain of the reflected light (red-shift) while displacement towards low wavelength (blue shift) is much less pronounced. The increase of the octahedral d-d band intensity (and so, absorption window enlargement for  $\text{LiCoPO}_4$ ) could be issued from the increase of the octahedral site distortion versus temperature: indeed, the thermal vibrations can induce the disappearance of the octahedral symmetry centre, leading to the increase of the d-d transition probability. The consequence is a progressive shift in colour of  $\text{LiCoPO}_4$  from dark pink to violet upon heating, the "blue" contribution being reinforced at the expense of the "red" one. Fig. 4 gathers photographs of  $\text{Bi}_2\text{O}_3$ ,  $\text{CoAl}_2\text{O}_4$  and  $\text{LiCoPO}_4$  at  $30^\circ\text{C}$  and  $200^\circ\text{C}$ .




**Table 1**  
Evolution of the Lab colorimetric parameters of  $\text{Bi}_2\text{O}_3$ ,  $\text{LiCoPO}_4$  and a  $\text{Bi}_2\text{O}_3/\text{LiCoPO}_4$  mixture with temperature.

$T(^{\circ}\text{C})$	$\sim 20^{\circ}\text{C}$	$100^{\circ}\text{C}$	$200^{\circ}\text{C}$
$L$	97	92	88
$a$	−6.5	−11.5	−14.5
$b$	24	58	81
Obtained colours			

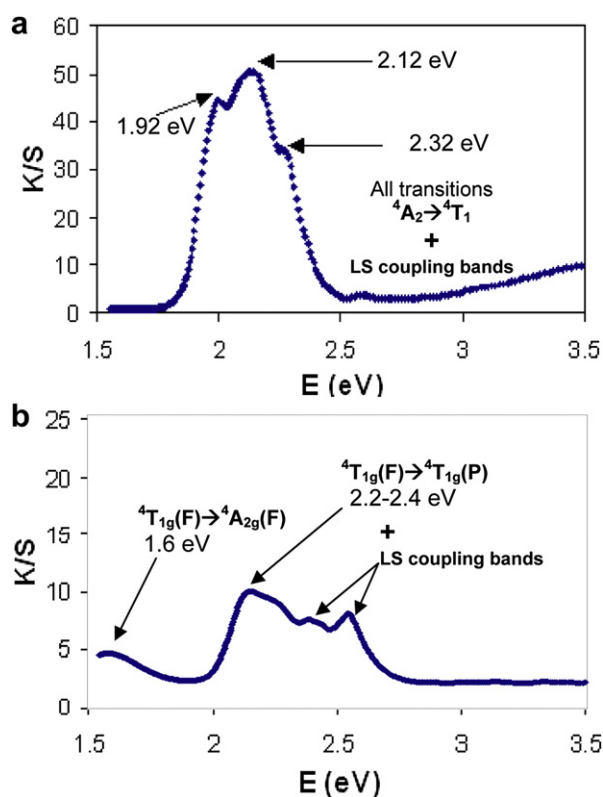
$T(^{\circ}\text{C})$	$\sim 20^{\circ}\text{C}$	$100^{\circ}\text{C}$	$200^{\circ}\text{C}$
$L$	41	39	37
$a$	34.5	31	28
$b$	−49.5	−48	−48
Obtained colours			

$T(^{\circ}\text{C})$	$\sim 20^{\circ}\text{C}$	$100^{\circ}\text{C}$	$200^{\circ}\text{C}$
$L$	55.5	53.5	49.5
$a$	8.9	2.2	−8.1
$b$	−1.0	0.1	0.8
Obtained colours			

Based on these observations, let us consider now the colour mixing law.

Since the  $\text{Bi}_2\text{O}_3$  semiconductor is pale yellow, its addition to a blue pigment as the spinel  $\text{CoAl}_2\text{O}_4$  (i.e. a pigment absorbing in



**Fig. 2.** Kubelka-Munk transformed reflectance spectra of (a)  $\text{CoAl}_2\text{O}_4$  and (b)  $\text{LiCoPO}_4$  intra-atomic transfer pigments.

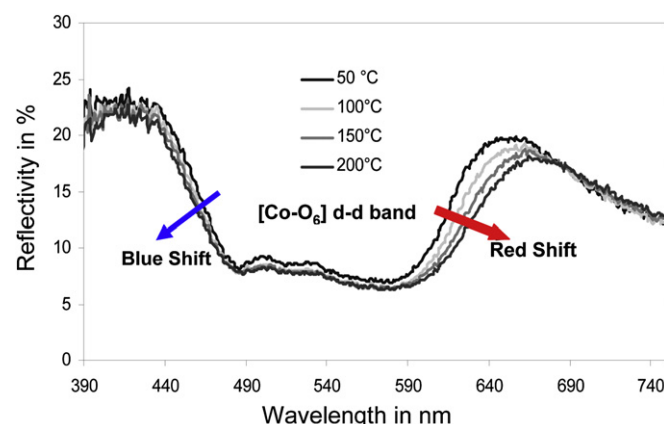


**Fig. 3.** Evolution of the reflectance spectra of  $\text{LiCoPO}_4$  versus temperature between room and  $200^{\circ}\text{C}$ .

the red-orange region), an unsaturated green colour can be achieved upon heating. Four  $\text{Bi}_2\text{O}_3/\text{CoAl}_2\text{O}_4$  mixtures were prepared with different mass ratios. Photographs of these blends at  $20^{\circ}\text{C}$  and  $200^{\circ}\text{C}$ , as well as a schematic representation of the colour evolution mechanism, are depicted in Fig. 5. As expected, the contrast can be adjusted at will by playing with the concentration of the precursors. At room temperature, the mixture absorbs only in the 1.6–2.4 eV region and above 2.8 eV leading to a blue-cyan colour. When temperature is raised, the absorption threshold of  $\text{Bi}_2\text{O}_3$  is displaced towards low energy, and only the "green light" is reflected. Actually, the red-shift of  $\text{Bi}_2\text{O}_3$  gap – about 0.2 eV between  $200^{\circ}\text{C}$  and room temperature –, induces an important decrease of the reflected blue wavelengths. Hence, even if the intrinsic colour change of  $\text{Bi}_2\text{O}_3$  oxide powder with temperature is not very important, the disappearance of the blue component of the  $\text{Bi}_2\text{O}_3$ – $\text{CoAl}_2\text{O}_4$  mixtures is drastically detected. A cyan → green → yellow sequence is then obtained for the  $\text{Bi}_2\text{O}_3$ – $\text{CoAl}_2\text{O}_4$  mixtures. Let us now replace the blue  $\text{CoAl}_2\text{O}_4$  pigment by the magenta  $\text{LiCoPO}_4$  one. Numerous mixtures of the two  $\text{Bi}_2\text{O}_3$  and  $\text{LiCoPO}_4$  compounds were made with various weight ratios. Fig. 6 shows the colour change in temperature of three  $\text{Bi}_2\text{O}_3/\text{LiCoPO}_4$  mixtures. An optimized composition (in terms of contrast) was established a 60 wt% of bismuth oxide composition but this choice strongly depends on the observer. The evolution of the Lab parameters of  $\text{Bi}_2\text{O}_3$ ,  $\text{LiCoPO}_4$  and the  $\text{LiCoPO}_4/\text{Bi}_2\text{O}_3$  optimal mixture is given in Table 1 with a coloured rectangle as reference. Again, it appears clear that the juxtaposition of a thermochromic semiconductor with a d-d temperature stable pigment strongly reinforced the colour change of the semiconductor alone. Indeed, in a quite restrict temperature range, the complete sequence pink → grey → green is observed. Actually, the efficiency of the mixture is dependent on subtractive colour system rules as for ruby compounds. Indeed, the optical contrast between room temperature and  $200^{\circ}\text{C}$ , calculated as  $\Delta E = (\Delta L^{*2} + \Delta a^{*2} + \Delta b^{*2})^{1/2}$ , is not stronger for the mixture than for the  $\text{Bi}_2\text{O}_3$  semiconducting powder alone. This observation only shows that the human eye is more sensitive to pink → green sequence than to the white → yellow sequence, even if these two sequences exhibit comparable optical contrasts. Here it can be reminded that as previously demonstrated, the historic observation of the thermochromism effect on ruby system is due to the eye sensitivity to the red to green translation via an achromatic hue (grey). However, the colour strength of the so-prepared mixing, where the overall absorption is related both to a charge transfers and d-d intra-atomic transitions, is significantly increased in comparison to ruby. Consequently, this opens up the door to the manufacturing of new thermochromic pigments with a large panel



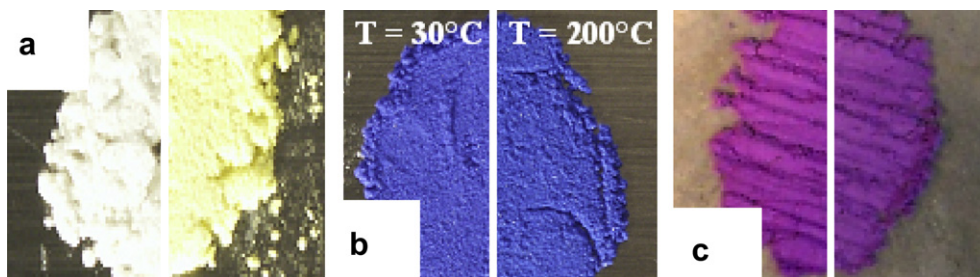


Fig. 4. Photographs of  $\text{Bi}_2\text{O}_3$ ,  $\text{CoAl}_2\text{O}_4$  and  $\text{LiCoPO}_4$  at room temperature and 200 °C.

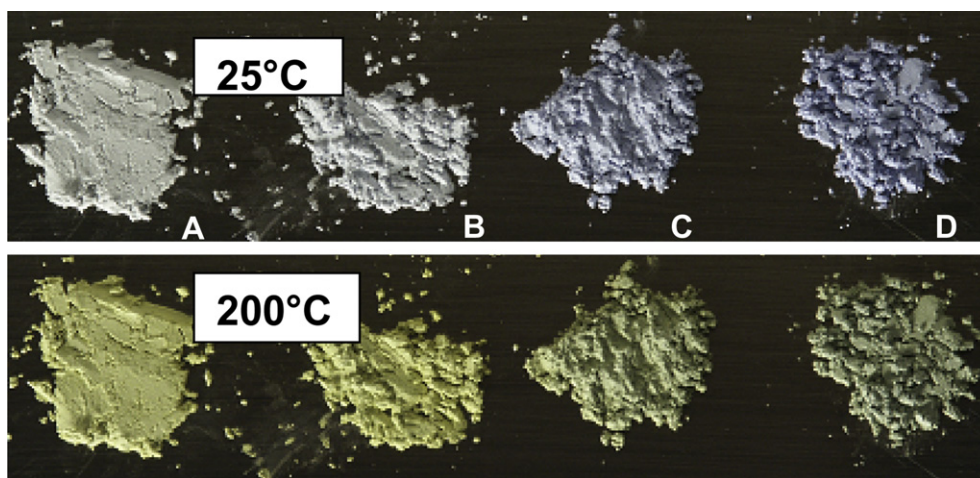


Fig. 5. Photographs of various  $\text{Bi}_2\text{O}_3/\text{CoAl}_2\text{O}_4$  mixtures at room temperature (top) and 200 °C (bottom) (the notation A, B, C and D corresponds to decreasing  $\text{Bi}_2\text{O}_3$  weight percentages).

of accessible colour and temperature transition domains. Typically, if we focused so far on the red to green transition by analogy with ruby, the opposite green to red transition can be envisioned by mixing an orange semiconductor (e.g.  $\text{V}_2\text{O}_5$ ) with a green pigment (e.g.  $\text{Cr}_2\text{O}_3$ ). Pictures of  $\text{V}_2\text{O}_5$ ,  $\text{Cr}_2\text{O}_3$  and  $\text{V}_2\text{O}_5/\text{Cr}_2\text{O}_3$  mixtures at 20 and 200 °C are given in Fig. 7 with an over-simplified model of the thermochromic effect.

This study is non exhaustive and numerous mixtures can *a priori* produce an emphasis effect of the colour switch of a thermochromic substance by an appropriate association with another pigment. By the way, the association of a thermochromic semiconductor with further crystal field pigments allows an infinite number of combinations thus thermochromic colourations which can be adjusted at will.

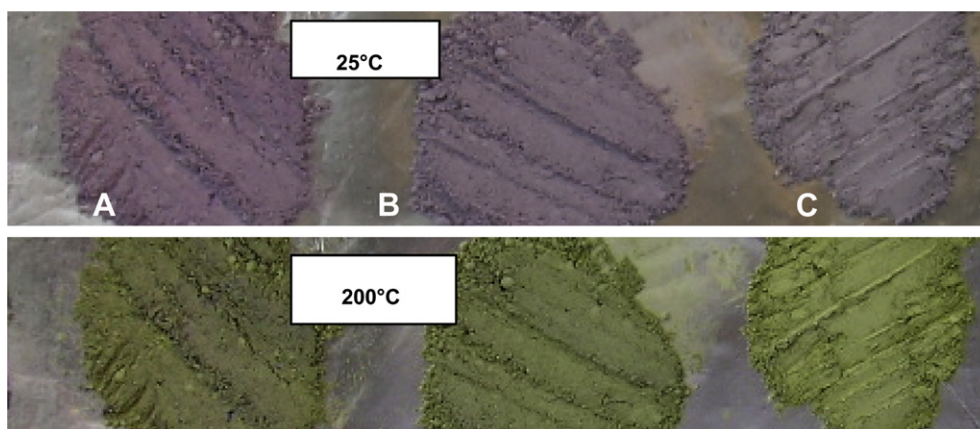
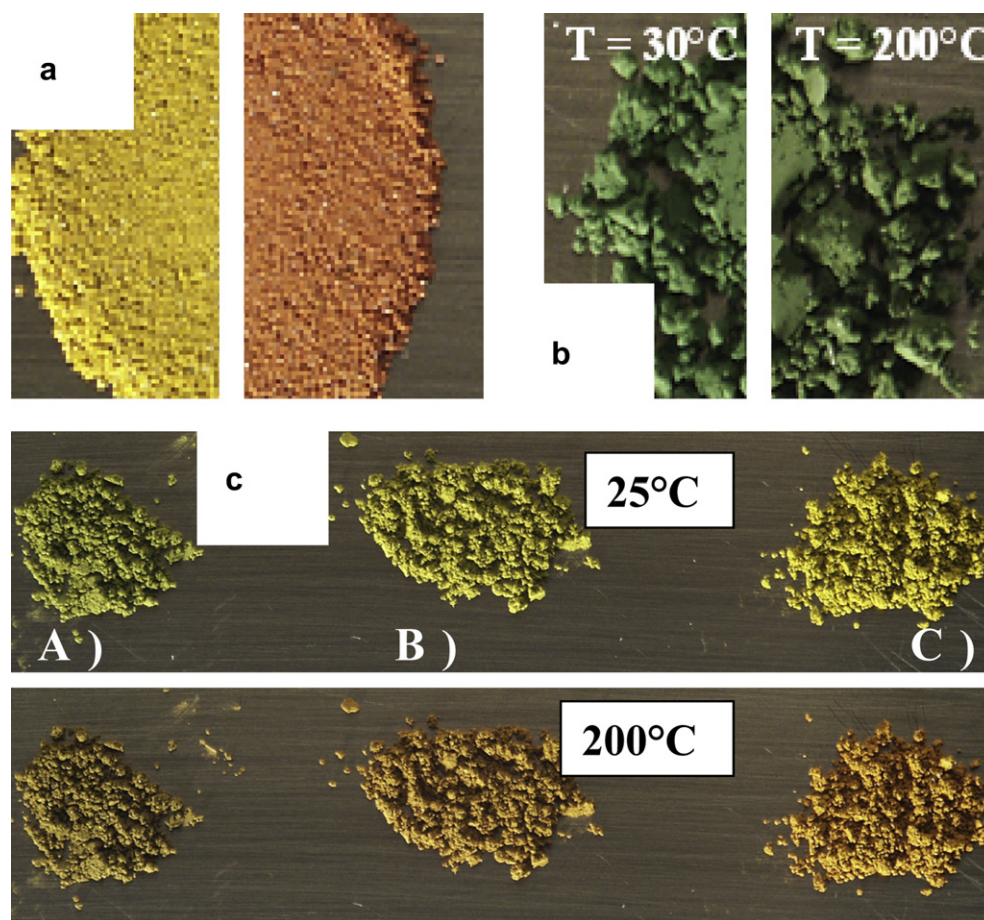


Fig. 6. Photographs of various  $\text{Bi}_2\text{O}_3/\text{LiCoPO}_4$  mixtures at room temperature (top) and 200 °C (bottom) (the notation A, B, and C corresponds to increasing  $\text{Bi}_2\text{O}_3$  weight percentages).



**Fig. 7.** Photographs of a)  $V_2O_5$ , b)  $Cr_2O_3$  and c) various  $V_2O_5/Cr_2O_3$  compositions at room temperature (top) and 200 °C (bottom) (the notation A, B and C corresponds to increasing  $V_2O_5$  weight percentages).

	room	200°C
A	R255 G255 B200	R255 G255 B000
B	R150 G075 B150 Trans.50%	R100 G075 B175 Trans.50%
A + B		

**Fig. 8.** How to easily produce with pastilles with the reported RGB parameters the as-ruby thermochromism of one semiconductor – crystal field pigment mixture (\*see tutorial of the supplementary file).

## 5. Conclusion

The large variation versus temperature of the band-gap of semiconductors was associated with an appropriate additional pigment (with colouration based on d-d transition) in order to obtain optimized and reversible thermochromic mixtures. The efficiency of the additional pigment was explained through the colour system rules, an analogy with the well known ruby system being chosen as a base for discussion. It can be proposed to the reader to perform on power point or other software the colour sequence reproduced on Fig. 8 to improve the demonstration. To produce such Fig. 8 colour sequence, one has to see the tutorial joined at the end of the paper. Finally, since an infinite number of mixtures can be prepared, it has to be noticed that this work opens the possibility to prepare an infinite palette of new thermochromic inorganic systems with improved optical contrast on shorter temperature range.

### 5.1. Tutorial

The Fig. 8 of the manuscript can be used as a tool in order to get new ideas to develop new pigments mixtures with high colour variation versus temperature. The principle is that a pigment mixture colour can be, in first approximation, easily simulated as the superimposition of two drawn squares (using a draw soft) with the one being back with 0% of transparency and the one being front with 50% of transparency.

With the Microsoft Power Point or Word softwares or equivalent,

- In the drawing tools bar, select the square shape and creates 6 equivalent squares as in the Fig. 8.
- On each square, in order to control the colour, press on the mouse' right button and define the shape colour using tab "more Fill Colours" item or "colour options" tab depending on the soft version.
- Enter the *R*, *G* and *B* desired levels for the each six squares.
- For the two *B* composition squares, thanks to the transparency bar, set the transparency to 50%.
- To get the two *A + B* squares (Fig. 8, third line) you have to fill the two squares with the same *R*, *G*, *B* values than for the two corresponding *A* compositions squares.
- Then copy and paste the two corresponding *B* composition squares on this *A + B* squares in respect of their column.
- Using various colours depending on your imagination/creativity, feel free to try to obtain a more drastic optical contrast between the two *A + B* squares trying in the same time, to decrease the optical contrast between the two *A* squares and the two *B* squares. In the case of you are happy with your own results; synthesize new inorganic pigments to reproduce experimentally your colour effect.

## References

- [1] Nassau K. *American Mineralogist* 1978;63:219.
- [2] Nassau K. In: *The physics and chemistry of color*. New-York: John Wiley & Sons; 2001.
- [3] Peter AL. In: *Pigment handbook*. New-York: John Wiley & Sons; 1987.
- [4] Sone K, Fukuda Y. *Inorganic thermochromism*. Berlin: Springer-Verlag Press; 1987.
- [5] Day JH. *Chemical Review* 1963;63:65.
- [6] Day JH. *Chemical Review* 1968;68:649.
- [7] Tilley RJD. *Color and optical properties of materials: an exploration of the relationship between light, the optical properties of materials and color*. Chichester: John Wiley & Sons Ltd; 1999.
- [8] Elias M, Lafait J. *Lumière, Vision et Matériaux*. Paris: Belin Ed; 2006.
- [9] Zuppiroli L, Bussac M-N. *Traité des Couleurs*. Paris: Broché; Ed; 2002.
- [10] Keiser PK, Boynton RM. *Human color vision*. Washington DC: Optical Society of America Ed; 1996.
- [11] Reinen D. *Structure and Bonding* 1969;6:30.
- [12] Burns RG. *Mineral applications of crystal field theory*. Cambridge: Cambridge University Press; 1993.
- [13] Xu G, Huang C-M, Jin P, Tazawa M, Chen D- M. *Journal of Applied Physics* 2008;104:5.
- [14] Kam KC, Cheetham AK. *Materials Research Bulletin* 2006;4:1015.
- [15] Qureshi U, Manning TD, Parkin IP. *Journal of Materials Chemistry* 2004;14: 1190.
- [16] Guinneton F, Valmalette J-C, Gavarri J-R. *Optical Materials* 2000;15:111.
- [17] Maaza M, Bouziane K, Maritz J, McLachlan DS, Swanepool R, Frigerio JM, et al. *Optical Materials* 2000;15:41.
- [18] Burkhardt W, Christmann T, Meyer BK, Niessner W, Schalch D, Scharmann A. *Thin Solid Films* 1999;345:229.
- [19] Livage J, Beteille F, Roux C, Chatry M, Davidson P. *Acta Materialia* 1998;46:743.
- [20] Gaudon M, Carbonera C, Thiry AE, Demourgues A, Deniard P, Payen C, et al. *Inorganic Chemistry* 2007;46:10200.
- [21] Gaudon M, Deniard P, Demourgues A, Thiry A-E, Carbonera C, Le Nestour A, et al. *Advanced Materials* 2007;19:3517.
- [22] Ehrenberg H, Weitzel H, Paulus H, Wiesmann M, Witschek G, Geselle M, et al. *Physic and Chemistry of Solids* 1997;58:153.
- [23] Wiesmann M, Ehrenberg H, Miede G, Peun T, Weitzel H, Fuess H. *Journal of Solid State Chemistry* 1997;132:88.
- [24] Rodríguez F, Hernández D, García-Jaca J, Ehrenberg H, Weitzel H. *Physical Review B* 2000;61:16497.
- [25] Thiry AE, Gaudon M, Payen C, Daro N, Létard J-F, Gorsse S, et al. *Chemistry of Materials* 2008;20:2075.
- [26] Gaudon M, Thiry AE, Largeteau A, Deniard P, Jobic S, Majimel J, et al. *Inorganic Chemistry* 2008;47:2404.
- [27] Kittel C. In: *Introduction to solid state physics*. New-York: John Wiley & Sons; 1995.
- [28] Madelung O. *Semiconductors — basic data*. Springer-Verlag Ed; 1996.
- [29] Streetman BG, Sanjay B. *Solid state electronic devices*. New-Jersey: Printice Hall Ed; 2000.
- [30] Mimani T, Ghosh S. *Current Science* 2000;78:892.
- [31] Russ NM, Kvyatkovskaya KK, Azarov VY, Bol'shova SP, Kosorukova ES. *Glass and Ceramics* 1989;45:242.
- [32] Corbeil M-C, Charland J-P, Moffatt EA. *Studies in Conservation* 2002;47:237.
- [33] Lever ABP. *Studies in physical and theoretical chemistry, inorganic electronic spectroscopy*. 2nd sub-ed. Elsevier Ed; 1985.
- [34] Meseguer S, Tena MA, Gargori C, Badenes JA, Llusar M, Monros G. *Ceramic International* 2007;33:843.
- [35] Gaudon M, Apheceixborde A, Ménétrier M, Le Nestour A, Demourgues A. *Inorganic Chemistry* 2009;48:9091.
- [36] Dai D, Whangbo M-H, Koo H-J, Rocquefelte X, Jobic S, Villesuzanne A. *Inorganic Chemistry* 2005;44:2407.
- [37] Deniard P, Dulac AM, Rocquefelte X, Grigorova V, Lebacq O, Pasturel A, et al. *Journal of Physics and Chemistry of Solids* 2004;65:229.
- [38] Gaudon M, Apheceixborde A, Ménétrier M, Demourgues A. *Inorganic Chemistry* 2010;46:10996.
- [39] Zayat M, Levy D. *Chemistry of Materials* 2000;12(2000):2763.